Applied Acoustics 202 (2023) 109184

Contents lists available at ScienceDirect

Applied Acoustics

journal homepage: www.elsevier.com/locate/apacoust

Design and optimization of micro-perforated ultralight sandwich structure with N-type hybrid core for broadband sound absorption

Yongfeng Jiang [a,b], Cheng Shen [a,b,*], Han Meng [a,b,*], Wei He [c], Tianjian Lu [a,b,*]

[a] State Key Laboratory for Mechanics and Control of Mechanical Structures, Nanjing University of Aeronautics and Astronautics, Nanjing 210016, PR China
[b] Nanjing Center for Multifunctional Lightweight Materials and Structures (MLMS), Nanjing University of Aeronautics and Astronautics, Nanjing 210016, PR China
[c] State Key Laboratory for Strength and Vibration of Mechanical Structures, Xi'an Jiaotong University, Xi'an 710049, PR China

ARTICLE INFO

Article history:
Received 25 September 2022
Received in revised form 11 December 2022
Accepted 19 December 2022
Available online 29 December 2022

Keywords:
Micro-perforated sandwich
Sound absorption
Multifunctionality
Lightweight
Optimization

ABSTRACT

We propose a novel ultralight multifunctional micro-perforated sandwich structure with N-type hybrid core, which exhibits excellent sound absorption as well as good load-bearing capacity and heat transfer performance. Sound absorption coefficient of the sandwich structure is calculated by establishing an analytical model. To validate the analytical model predictions, both experimental measurements and numerical simulations are carried out, with good agreement achieved. Physical mechanisms leading to the excellent acoustic performance of the structure are revealed, and effects of geometric parameters are quantified. For maximized sound absorption at minimal structural weight, an optimization strategy is developed with the Simulated Annealing algorithm. Compared with non-optimal sandwich structures, the optimal structure enables reduced weight and better absorption within broader frequency range. The proposed ultralight sandwich structure with integrated multifunctional attributes has significance in engineering applications demanding excellent mechanical, thermal, acoustic performances as well as low mass and volume.

1. Introduction

Lightweight multifunctional structures have become important in numerous engineering fields, particularly so in aerospace industry. For instance, aircraft engine casings and rocket fairings in extreme working environment such as high sound pressure and temperature require structures that are low weight and exhibit great load bearing, energy absorption, heat dissipation and sound insulation properties. In recent years, sandwich structures with ordered macroporous cores (e.g., highly porous lattice trusses) have emerged as excellent multifunctional lightweight structures, thus attracting tremendous attention in the fields of mechanics, heat transfer, material design, energy absorption, and the like [1–12]. For example, sandwich structures with corrugation and I-section cores are typical ultralight structures with multifunctional attributes (e.g., load bearing, energy absorption and active cooling) that have found a variety of applications such as bridge/ship decks and high-speed train bodies [4,13–20]. Nonetheless, for ground transportation vehicles demanding even higher speeds (>1000 km/h) and aerospace applications, both types of sandwich structure need further improvement in load support and multifunctionality: while a sandwich with corrugation core generally has superior load-bearing capacity to the one with I-section core, it tends to buckle with small strains in out-of-plane compression [21]. To squarely address the deficiency of both sandwich core types in structural load-bearing, in a recent study [22], we integrated the I-sections and corrugations to construct a N-type hybrid (NH) core, and demonstrated significantly enhanced resistance of the resulting sandwich to buckling [22]. Besides, the sandwich structures with NH cores were also found to have better heat transfer performance of the NH-cored sandwich relative to that with corrugation core [23–26].

Gaining insight from micro-perforated panels (MPPs) proposed by Maa in 1975 [27], incorporating micro perforations into sandwich structures can lead to improved sound absorption without greatly affecting their mechanical and thermal attributes. Typically, a MPP contains submillimeter to millimeter perforations with either smooth or roughened surfaces, which form multiple Helmholtz resonators that exhibit excellent sound absorption in vicinity of the resonance frequency. The MPP is environmental-friendly, flexible in design, convenient in manufacture and low in cost, thus has been widely used as walls and ceilings in buildings,

* Corresponding authors at: State Key Laboratory for Mechanics and Control of Mechanical Structures, Nanjing University of Aeronautics and Astronautics, Nanjing 210016, PR China.
E-mail addresses: cshen@nuaa.edu.cn (C. Shen), menghan@nuaa.edu.cn (H. Meng), tjlu@nuaa.edu.cn (T. Lu).

https://doi.org/10.1016/j.apacoust.2022.109184
0003-682X/

construction equipment, mufflers, etc. [28–34]. However, despite of its attractive acoustic performance, the MPP is essentially not designed for load-bearing, energy absorption, thermal management and the like.

Combining the MPP with sandwich-like structures to construct multifunctional structures has thus emerged. For instance, the sound performances of MPP-air cavity-plate systems were investigated using experimental and analytical methods. Compared with MPPs, the combined sandwich structures demonstrated both effective sound absorption and insulation [35–37]. Meng et al. [38,39] developed micro-perforated sandwich panel with either honeycomb or corrugation core and demonstrated that the micro-perforated sandwich structure exhibited significant improvement in both sound transmission loss and sound absorption. In particular, Tang et al. [40–42] proposed a sandwich structure with honeycomb-corrugation hybrid core and embedded micro perforations in the face panel and core. They investigated the sound absorption performances of the micro-perforated structure at normal temperature and pressure as well as extreme environment (i.e., high temperatures and sound pressure) and found that the micro-perforated structures can maintain good sound absorption properties in low frequency range as well as excellent load carrying and energy absorption capacity regardless of the ambient environment. He et al. [43] proposed a micro-perforated sandwich structure with multilayer hierarchical honeycomb core, and demonstrated that the combination of micro perforations and laminated honeycomb core lead to multiple peaks in the sound absorption curves, hence broadened the sound absorption band.

Inspired by the abovementioned micro-perforated structures, micro perforations are added in the sandwich structure with NH core in the paper to obtain good sound absorption. It should be noted that the multifunctionality of perforated honeycomb-corrugation hybrid cored sandwich panels in Refs. [40–42] lies in mechanical (compressive strength, energy absorption capacity, etc.) and sound absorption attributes, whereas the multifunctionality of NH cored sandwich structures is demonstrated as good heat transfer performance and sound absorption as well as load support. Moreover, different from the abovementioned structures with micro perforations of identical dimensions, the sandwich structure with NH core in the present paper has micro perforations of varying diameters in both the facesheet and NH core for the purpose of broadening the sound absorption further. The sound absorption coefficient of the micro-perforated sandwich structure is calculated by an electric-acoustic analogy analytical model, which is subsequently verified by numerical simulation and experiment. The sound absorption mechanisms of the micro-perforated sandwich structure with NH core are later explored based on the numerical simulation model. Influences of the micro perforations are explored by comparison with other sandwich structures, the effects of key geometric parameters on the sound absorption performance of the structure are also discussed. As the sound absorption coefficient changes dramatically with the geometric parameters, an optimization strategy is proposed after that to search for the optimal geometric parameters that both maximize the sound absorption performance at targeted frequencies and minimize the mass of the structure by virtue of the simulated annealing algorithm.

The paper is structured as follow: Section. 2 introduces the analytical model for the sound absorption coefficient calculation of the micro-perforated sandwich structure with NH core. Verification of the analytical model is presented in *Sec*. 3. Section. 4 discusses the sound absorption mechanisms of the proposed sandwich structure and effects of micro perforations and geometric parameters on the sound absorption coefficient. Section. 5 introduces the optimization strategy for the proposed sandwich structure. Conclusions are given in *Sec*. 6.

2. Analytical model

The proposed micro-perforated sandwich structure with NH core is shown schematically in Fig. 1(a), it consists of micro-perforated upper facesheet, N-type hybrid core, and a non-perforated lower facesheet. The NH core is formed by I-section insertions and corrugation which are rigidly connected at the folding points as can be seen from Fig. 1(b). A unit cell of the proposed sandwich structure is shown in Fig. 1(c) with a length of a and a width of b. The height of NH core is D. The thicknesses of the facesheets, I-section insertions and corrugation core are t_f, t_v, t_c, respectively. $d_{mn}(m,n=1,2)$ denotes the diameters of the two micro perforations in the facesheet and NH core, respectively. It should be noted that, the micro perforations in the facesheet and corrugation core were generally uniform in previous research [40–43], the micro perforations are set with different diameters in the present paper for the purpose of expanding the sound absorption band.

The proposed micro-perforated sandwich structure with NH core can be regarded as series–parallel combination of Helmholtz resonant cavities with different resonant frequencies. The acoustic properties of the micro-perforated NH core are equivalent to that of a plate containing perforations of the same dimensions parallel to the facesheets [41], the sound absorption of the proposed micro-perforated sandwich structure can therefore be modeled by sandwich structure with parallel and vertical plate insertions as shown in Fig. 2(b). The I-section insertion separates the unit cell into two parallelly connected double-layered micro-perforated sandwich structures. D_1 and D_2 are the equivalent upper and lower cavity height, which can be calculated by the volumes and surface areas of cavities, as

$$D_1, D_2 = \frac{\frac{1}{2}\left(\frac{a}{2} - t_v - \frac{t_c}{2\sin\theta}\right)\left(D - \frac{t_c}{2\cos\theta}\right)}{\frac{a}{2} - t_v} \tag{1}$$

where θ is the angle between the corrugation and facesheet.

The impedance of each micro perforation in Fig. 2(b) under normal incidence can be according to Maa's model [27,44], as

$$Z_{mn}^{MP} = \frac{j\omega\rho_0 t_q}{p_{mn}}\left[1 - \frac{2}{x_{mn}\sqrt{-j}}\frac{B_1\left(x_{mn}\sqrt{-j}\right)}{B_0\left(x_{mn}\sqrt{-j}\right)}\right]^{-1} + \frac{\sqrt{2}\mu x_{mn}}{p_{mn}d_{mn}} + \frac{0.85j\omega\rho_0 d_{mn}}{p_{mn}} \tag{2}$$

where $m,n=1,2$, $q=f,c$, p_{mn} is the perforation ratio, $x_{mn}=d_{mn}\sqrt{\omega\rho_0/\mu}/2, j=\sqrt{-1}$ is the imaginary unit, ω is the angular frequency, $\rho_0=1.2\mathrm{kg/m^3}$ is the density of air, $\mu=1.85\times10^{-5}\mathrm{Pa\cdot s}$ is the viscosity coefficient of air, B_0 and B_1 are the zeroth and first order Bessel function of the first kind, respectively.

For the equivalent double-layered micro perforated panels shown in Fig. 2(b), the impedance could be calculated by [45]

$$\tilde{Z}_n = Z_{1n}^{MP} + Z_{D_1} + \frac{\left(Z_{D_1}\right)^2}{Z_{D_1} + Z_{D_2} + Z_{2n}^{MP}} \tag{3}$$

where $n=1,2$, $Z_{D_1} = -j\rho_0 c_0 \cot(\omega D_1/c_0)$, $Z_{D_2} = -j\rho_0 c_0 \cot(\omega D_2/c_0)$, Z_{1n}^{MP} and Z_{2n}^{MP} can be estimated according to Eq. (2). Given the influences of the thickness I-section insertions on the surface area, a correction factor is introduced to the impedance of the sandwich structure, as

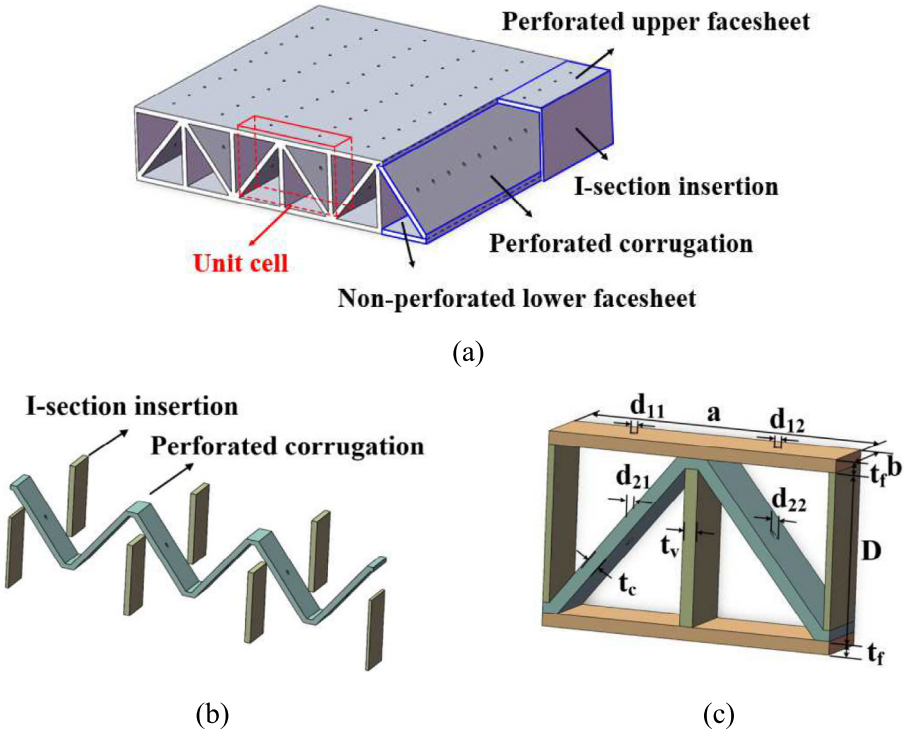

Fig. 1. Schematic diagrams of (a) the micro-perforated sandwich structure with NH core, (b) decomposition of NH core, and (c) a unit cell.

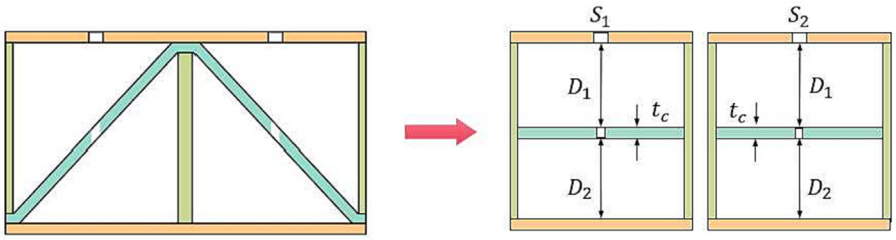

Fig. 2. Front view of the unit cell of the micro-perforated sandwich structure with NH core and equivalent simplified model of the unit cell.

$$Z_n = \tilde{Z}_n \, \delta_n \tag{4}$$

where $n = 1, 2$, $\delta_n = S_n / S_n^{eff}$, $S_n = ab/2$ is the surface area of the left and right part of the sandwich structure as shown in Fig. 2, $S_n^{eff} = (a/2 - t_v)b$ is the corrected surface area.

With regard to the two parallelly connected double layered micro-perforated sandwich structure, the total impedance can be calculated by

$$Z_T = \frac{1}{\sum_{n=1}^{2} \frac{S_n}{Z_n \times (S_1 + S_2)}} \tag{5}$$

The sound absorption coefficient of the micro-perforated sandwich structure with NH core is given by

$$\alpha = 1 - \left| \frac{z_s - 1}{z_s + 1} \right|^2 \tag{6}$$

where $z_s = Z_T / \rho_0 c_0$ is the relative surface impedance.

3. Verification

The analytical model is validated by both experiment and finite element (FE) simulation in this section.

The FE model of the micro-perforated sandwich structure with NH core is established by using COMSOL Multiphysics. For an infinite sandwich structure, the FE model is set up with a representative unit cell with periodic boundary as shown in Fig. 3. As the stiffness of the structure is much larger than that of the air, only the air domains inside the structure are considered in the model. The air domains are modeled by Thermoviscous Acoustics Module which takes the thermal conductivity and viscosity of the air into consideration. A plane wave is added in the background sound field. A perfectly matched layer (PML) that can absorb all the entered sound energy is set adjacent to the background sound field to create a non-reflection boundary. No-slip, isothermal boundary conditions are employed at the air-structure interferences, as

$$\begin{aligned} \boldsymbol{u} &= 0 \\ T &= 0 \end{aligned} \tag{7}$$

where $\boldsymbol{u}$ and T are the velocity and temperature rise at the air-structure interferences. The surface impedance of the sandwich structure is calculated by

$$Z_s = \frac{\langle p_z \rangle_s}{\langle v_\perp \rangle_s} \tag{8}$$

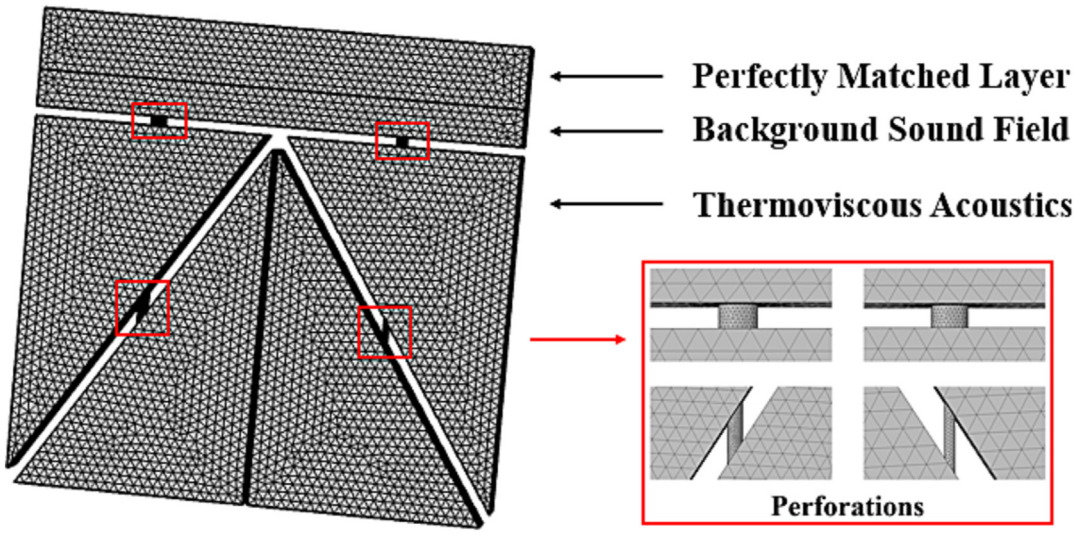

Fig. 3. Numerical simulation model of the micro-perforated sandwich structure with NH core in COMSOL Multiphysics.

where $\langle p_z \rangle_s$ and $\langle v_\perp \rangle_s$ are the averaged sound pressure and vertical velocity at the surface respectively. The sound absorption coefficient of the sandwich structure can then be obtained by substituting Eq. (8) to Eq. (6).

The sound absorption coefficient of sandwich structure with NH core was measured by the SW101-L/SW100-S acoustic testing system. Fig. 4 show the photo and schematic diagram of the experimental device. The inner side length of the impedance tube is 100 mm, the measuring frequency range is 200 Hz–1600 Hz. The experimental sample with dimensions of 100mm$\times$ 100mm $\times$ 34mm was made of resin with a density of 1.117 g/cm^3 and prepared by stereo lithography 3D printing technology. Photo of the printed sample is shown in Fig. 5. Geometric parameters of the sample are listed in Table 1.

The sound absorption coefficient obtained by analytical prediction and numerical simulation is compared in Fig. 6(a). It can be seen from Fig. 6(a) that, the analytical results show reasonable agreement with the numerical results, the two curves show the same trends, and the sound absorption peaks occur at similar frequencies. The differences between the analytical and numerical results may be caused by the simplifications and assumptions of the analytical model. That is, the analytical model adopts the equivalent double layer micro-perforated panel method, which is different from the actual sandwich structures with NH cores in the numerical models. The numerical models also take both the viscous and thermal energy dissipation into consideration, whereas the analytical model considers only the viscous energy dissipation. Comparison between the analytical and experimental results is shown in Fig. 6(b). It can be seen from Fig. 6(b) that the analytical results agree well with the experimental results, the sound absorption peaks occur at identical frequencies and the curves have the same trends. The discrepancies between the analytical prediction and experimental measurement may be attributed to non-ideal experimental conditions in the experiment. For instance, dimension errors and surface roughness of micro perforations could be introduced into the tested samples by the 3D printing manufacturing which would cause differences between simulation and experiment. Besides, the experimental results are obtained based on ideal plane wave propagation in the impedance tube, which is hard to achieve in real experiment process.

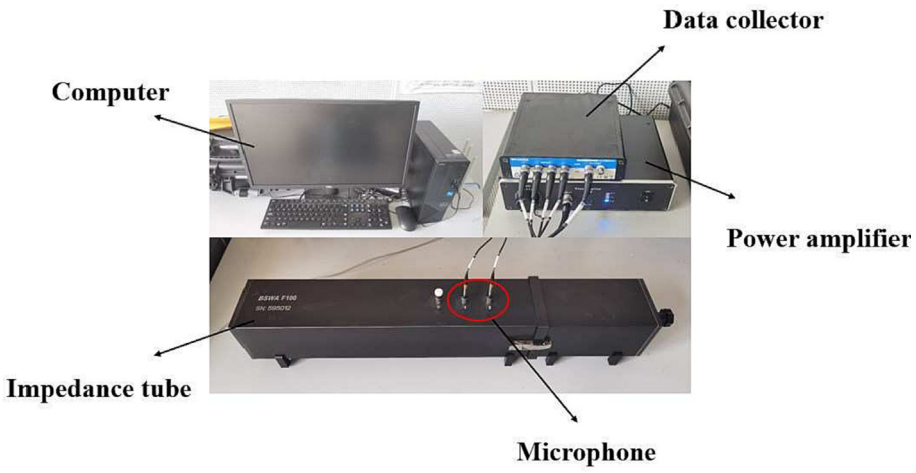

Fig. 4. (a) Photo and (b) schematic diagram of the SW101-L/SW100-S acoustic testing device.

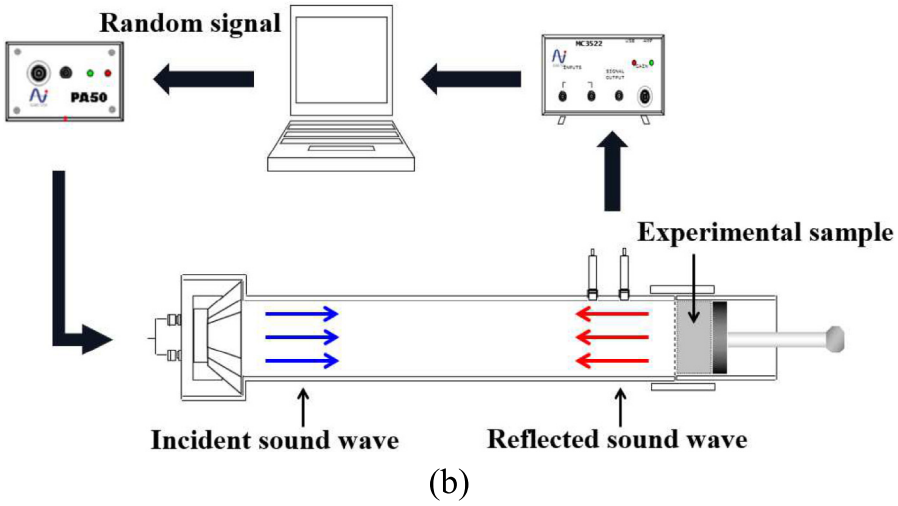

Fig. 4 (*continued*)

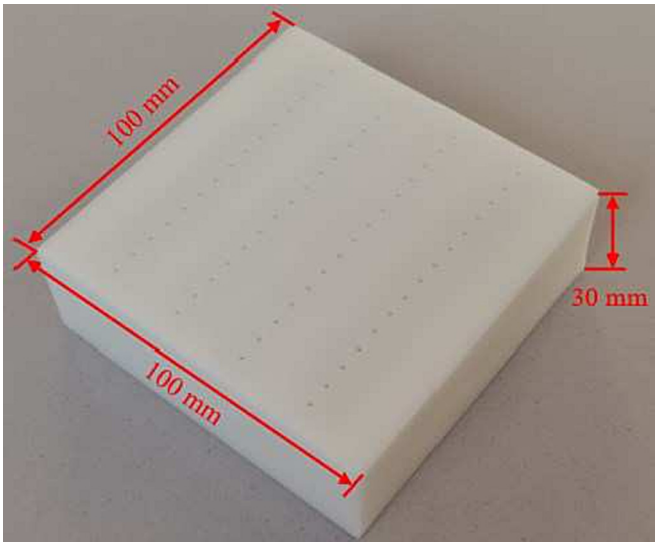

Fig. 5. Photo of the tested micro-perforated sandwich structure with NH core.

4. Results and discussion

4.1. Analysis of sound absorption mechanism

As is known, two energy dissipation mechanisms exist in micro-perforated structures, namely viscous energy dissipation and thermal energy dissipation due to the existence of viscous and thermal boundary layers. The sound absorption mechanism of the proposed sandwich structure with NH core is explored by the FE models in this subsection. FE models can not only verify the analytical model, it also reveals the underlying sound absorption mechanism due to the excellent visualization of energy dissipation.

Fig. 7 shows the viscous, thermal and total viscous-thermal energy dissipation power density inside the sandwich structure with NH core around the first resonance frequency at 500 Hz. The geometric parameters of the sandwich structure are the same as that listed in Table 1. It can be seen from Fig. 7 that the viscous energy dissipation is concentrated at the micro perforations, while the thermal energy dissipation distributes at the air-structure interferences. The amplitude of the viscous energy dissipation is also much larger than that of the thermal energy dissipation. The integrated viscous, thermal and total energy power dissipation in a unit cell of the sandwich structure is further compared in Fig. 8 (a) to have a deeper understanding of the sound absorption mechanism. It can be seen from Fig. 8(a) that the viscous power dissipation curve is almost coincided with the total power dissipation curve, while the thermal dissipation is much lower than the viscous dissipation, which means that the viscous effect dominates in the sound absorption of the micro-perforated sandwich structure.

The proportions of viscous and thermal energy dissipation in the total energy dissipation are plotted in Fig. 8(b). The viscous energy dissipation accounts for over 95 % of the total energy dissipation at frequencies around the resonance frequencies, i.e., over 400 Hz in the present figure. The proportion of viscous energy dissipation decreases gradually to about 80 % as the frequency deviates from the resonance frequencies, i.e., 200 $\sim$ 400 Hz. As is known, the air in the micro perforations vibrates fiercely at the resonance frequencies, which would enhance the viscous energy dissipation and lead to sound absorption. The viscous energy dissipation is thus maximized at the resonance frequencies. It is worth noting that only the viscous effect was considered in the classical Maa's MPP model mentioned in the last section, the thermal effect was actually ignored. The above analysis justifies the assumptions and simplifications in Maa's model for the sound absorption calculation.

Table 1
Geometric parameters of the tested micro-perforated sandwich structure with NH core sample (/mm).

a	b	t_f	t_c	t_v	d_{11}	d_{12}	d_{21}	d_{22}	D
40	6	2	2	2	1.5	1.5	1	1	30

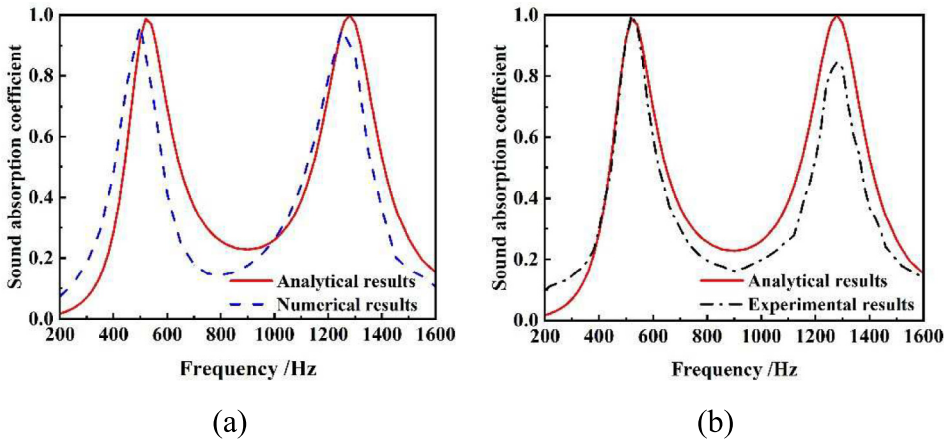

Fig. 6. Comparison of the sound absorption coefficient between the analytically predicted and (a) numerical, (b) experimental results.

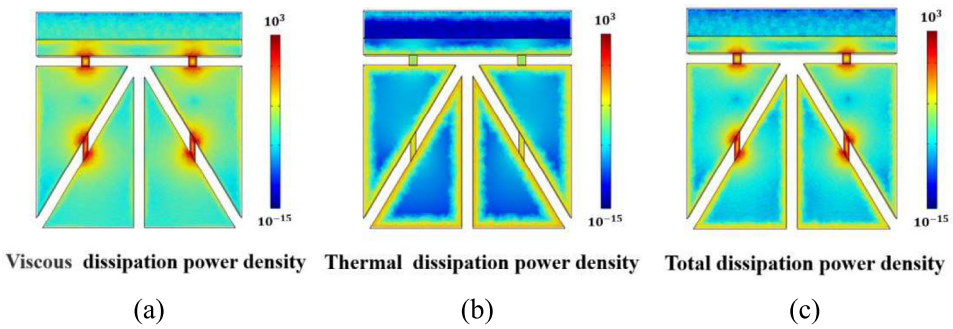

Fig. 7. Contour of the viscous, thermal, and total power dissipation density (W/m^3) at central sectional plane of the sandwich structure with NH core at 500 Hz, (a) viscous dissipation, (b) thermal dissipation, (c) total viscous-thermal dissipation.

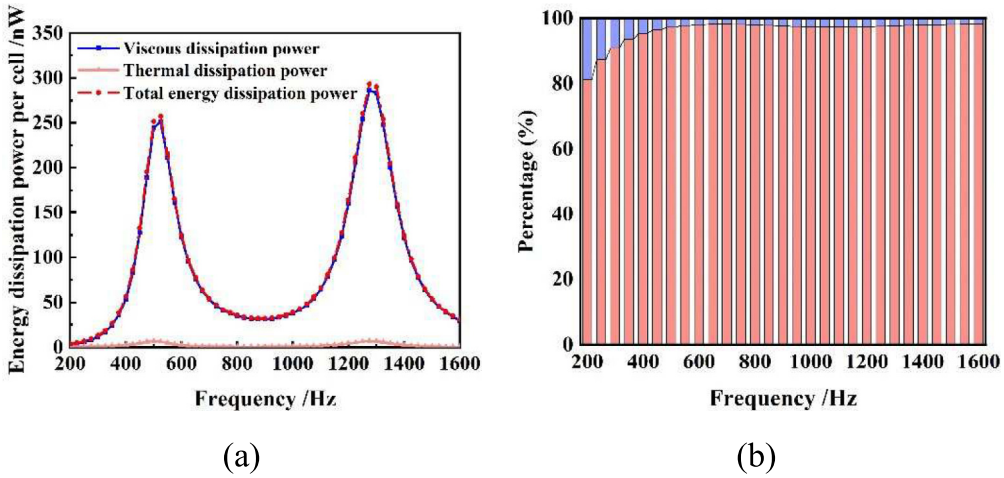

Fig. 8. (a) Comparison of thermal, viscous and total power dissipation in one unit cell, (b) proportions of thermal and viscous energy dissipation in the total energy dissipation. The lower part of the bars (in red) depicts the ratio of viscous energy dissipation and the upper part (in blue) shows the ratio of thermal energy dissipation. (For interpretation of the references to colour in this figure legend, the reader is referred to the web version of this article.)

4.2. Influences of micro perforations

The influences of micro perforations on the sound absorption of the sandwich structure with NH core are explored in this subsection. The sound absorption coefficient of the micro-perforated sandwich structure with perforated NH core is compared with that of the micro-perforated sandwich structure with non-perforated NH core and I-section core and of the same dimensions in Fig. 9. The geometric parameters of the sandwich structures are listed in Table 2.

It can be seen from Fig. 9 that the micro-perforated sandwich structure with perforated NH core has broader sound absorption compared with other structures, it has more peaks on the sound absorption curve due to resonances by multiple perforations with different diameters. Besides, the micro-perforated sandwich structure with perforated NH core has an averaged sound absorption

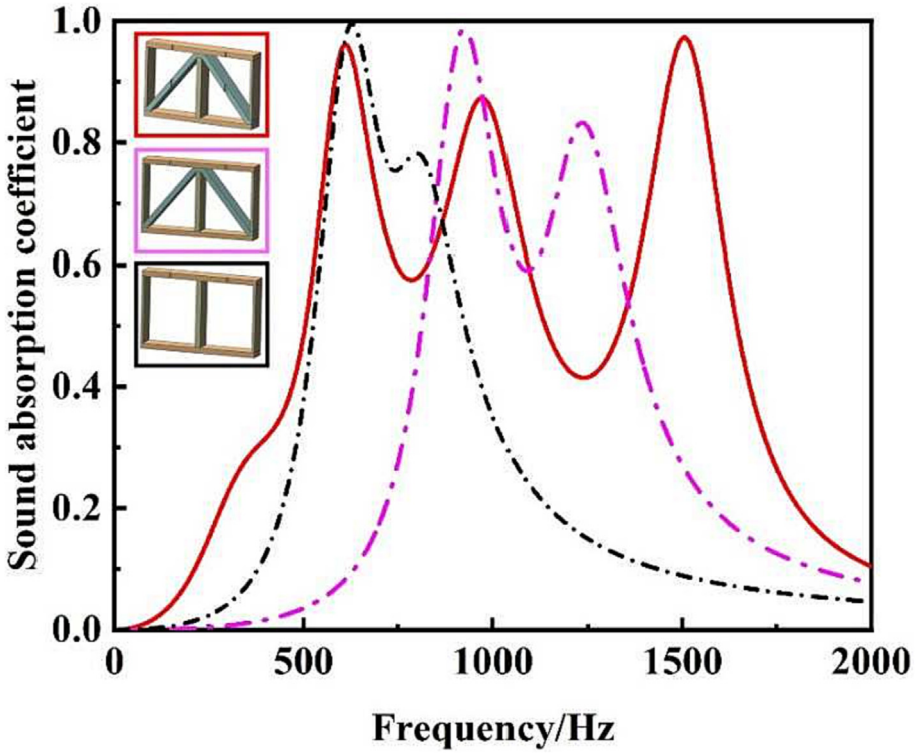

Fig. 9. Comparison of sound absorption coefficient of micro-perforated sandwich structures with perforated NH core (in red), non-perforated NH core (in magenta) and I-section core (in black). (For interpretation of the references to colour in this figure legend, the reader is referred to the web version of this article.)

Table 2
Geometric parameters of the micro-perforated sandwich structures with different cores (/mm).

	a	b	t_f	t_c	t_v	d_{11}	d_{12}	d_{21}	d_{22}	D
Perforated NH core	40	4	0.8	1.2	0.4	1.2	0.8	0.8	0.4	30
Non-perforated NH core	40	4	0.8	1.2	0.4	1.2	0.8	/	/	30
I-section core	40	4	0.8	/	0.4	1.2	0.8	/	/	30

coefficient of 0.486 in the frequency range of 0–2000 Hz, which is much higher than that of the other two structures with average values of 0.292 and 0.251 respectively. The micro-perforated sandwich structure with NH core is therefore a multifunctional lightweight structure with broadband sound absorption performances as well as excellent mechanical and thermal properties as mentioned above.

4.3. Effect of geometric parameters on sound absorption

In order to investigate the effects of key geometric parameters on the sound absorption performance of the structure, the sound absorption coefficients of sandwich structures with different unit cells and micro perforations are compared in this subsection based on the proposed analytical model.

Fig. 10 (a)-(d) compare the sound absorption coefficients of micro-perforated sandwich structures with different unit cell lengths and widths, core heights and panel thicknesses respectively. The geometric parameters of the sandwich structures are shown in Table 3. It can be seen from Fig. 10 that the absorption coefficient of the structure has a shift to the lower frequency with the increase of the unit cell length, width and the core height and the decrease of the I-section insertion thickness. As these changes could lead to an increase in the volume of the cavity in the sandwich structure, the low frequency sound absorption is therefore improved.

Except from parameters affecting the cavity volume mentioned above, the effects of micro-perforation dimension on the sound absorption performance of the structure are also investigated. Comparison of sound absorption coefficient of the structures with varying micro perforation dimensions is shown in Fig. 11. The other geometrical parameters correspond to that given in Table 3. It can be seen from Fig. 11 that the sound absorption peaks shift to higher frequency with the increased micro perforation diameters as the resonance frequency grows with the dimension of micro perforation. Besides, it can also be seen that the resonance peaks are determined by different micro perforations, the peaks at around 600 Hz and 1600 Hz are determined by the micro perforations in the left part of the unit cell, while other peak are decided by the micro perforations in the other part of the unit cell.

It can therefore be concluded from Figs. 10 and 11 that the micro-perforated sandwich structure has a high level of designability and flexibility with multiple designable geometrical parameters, it is therefore worth exploring the suitable geometrical parameters to meet different noise control needs in engineering applications.

5. Optimization

Since the sound absorption changes greatly with the geometric parameters as discussed in the last section, the sound absorption can be tuned by altering the geometric parameters, the geometric

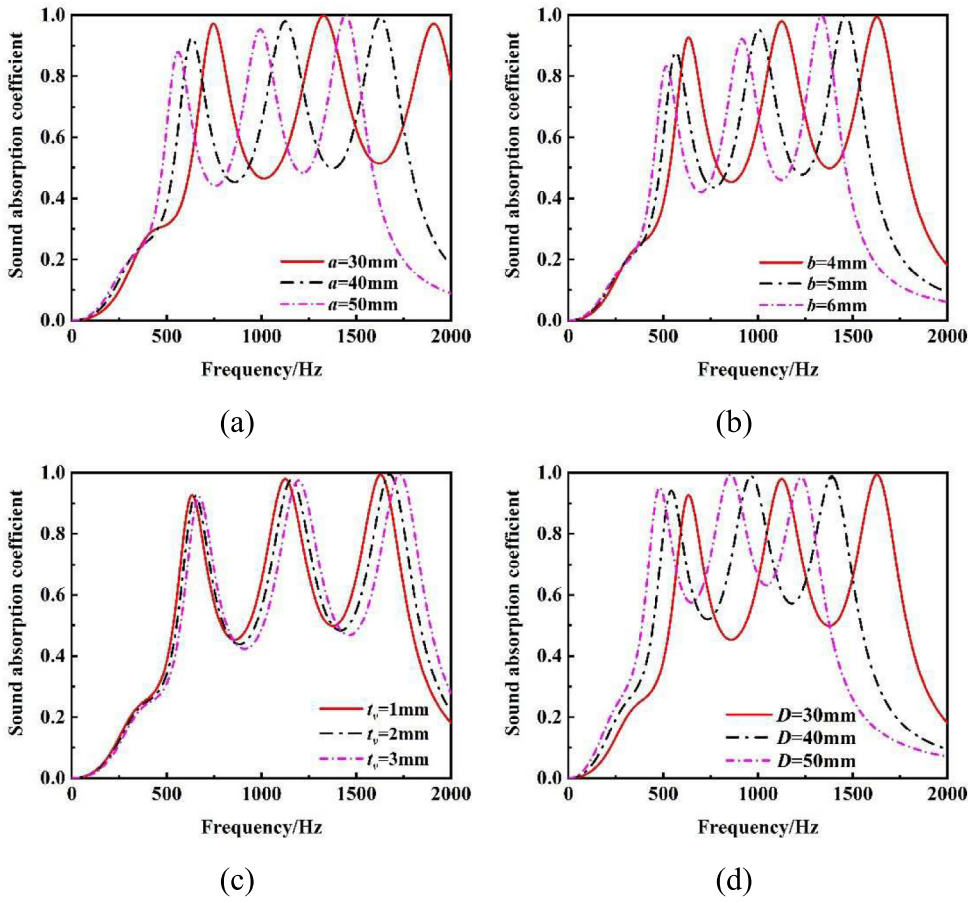

Fig. 10. Effects of geometric parameters on sound absorption of micro-perforated sandwich structures with NH core, (a) unit cell length $a = 30\text{mm}, 40\text{mm}, 50\text{mm}$; (b) unit cell width $b = 4\text{mm}, 5\text{mm}, 6\text{mm}$; (c) I-section thickness $t_v = 1\text{mm}, 2\text{mm}, 3\text{mm}$; (d) core height $D = 30\text{mm}, 40\text{mm}, 50\text{mm}$. The other geometric parameters are listed in Table 3.

Table 3
Geometric parameters of micro-perforated sandwich structures with NH core (/mm).

a	b	t_f	t_v	D	t_c	d_{11}	d_{12}	d_{21}	d_{22}
40	4	0.5	0.4	30	1.5	1.2	0.8	0.8	0.4

parameters are thus optimized in this section to maximize sound absorption performance and minimize the structural mass.

5.1. Optimization method

The optimization objective function taking both the sound absorption and mass of the sandwich structure into consideration is set up, as,

$$\max f(\boldsymbol{X}, \boldsymbol{\varphi}) = \frac{\int_{f_1}^{f_2} (\propto) df / M}{f_2 - f_1} \tag{9}$$

$$s.t. \boldsymbol{X}_{min} \le \boldsymbol{X} \le \boldsymbol{X}_{max}$$

where $\boldsymbol{X} = [a, b, t_f, t_c, t_v, d_{11}, d_{12}, d_{21}, d_{22}]$ denotes the geometric parameters for design, $\boldsymbol{X}_{min}$ and $\boldsymbol{X}_{max}$ are the lower and upper limit of $\boldsymbol{X}$. $\boldsymbol{\varphi} = [f_1\ f_2]$ is the targeted frequency range. $\propto$ is the sound absorption coefficient of the structure that can be calculated by Eq. (6). M denotes the relative mass of the structure, that is, the ratio of the mass of the structure to the total volume of the structure and internal air cavity, given as

$$M = \frac{(2at_f + 2Dt_v + 2S)b - \pi t_f \left[\left(\frac{d_{11}}{2}\right)^2 + \left(\frac{d_{12}}{2}\right)^2\right] - \frac{\pi t_c}{\cos\theta}\left[\left(\frac{d_{21}}{2}\right)^2 + \left(\frac{d_{22}}{2}\right)^2\right]}{[a \times b \times (D + 2t_f)]} \tag{10}$$

where S is the cross-sectional area of each subunit corrugation,

$$S = 2\left(\sqrt{D^2 + \left(\frac{a}{2} + t_v\right)^2} - \frac{t_c}{\tan\theta} - t_c \times \tan\theta\right) \times t_c + \frac{{t_c}^2}{\tan\theta} + {t_c}^2 \times \tan\theta \tag{11}$$

Simulated annealing algorithm is employed to solve the above optimization problem. Simulated annealing algorithm is a probabilistic optimization method used to approximate the global extreme values. The name of simulated annealing came from the annealing progress in metallurgy which includes heating a material to annealing temperature and then slowly cooling it down to gain desired properties and minimize the system energy. The simulated annealing algorithm not only has the advantages of easy implementation and strong robustness, it is also very useful for functions with multiple local minima for which algorithms like

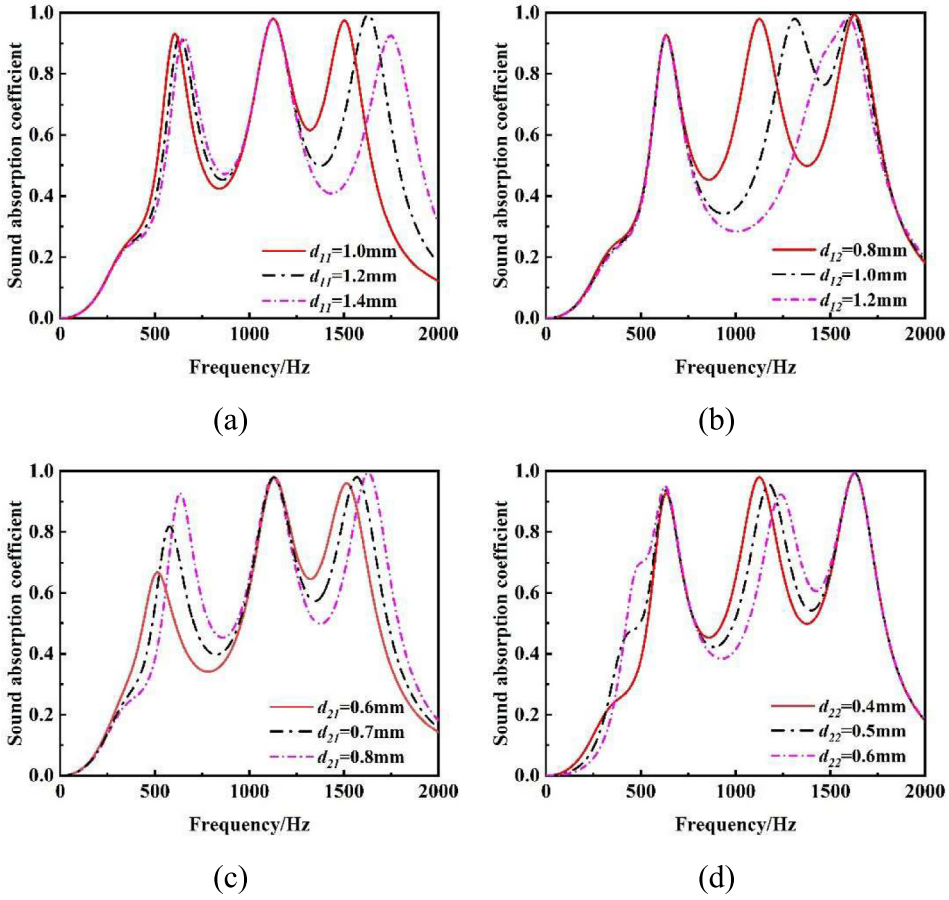

Fig. 11. Effect of micro perforation dimensions on sound absorption coefficient of the micro-perforated sandwich structures with NH core, (a) d_{11} = 1.0mm, 1.2mm, 1.4mm, (b) d_{12} = 0.8mm, 1.0mm, 1.2mm, (c) d_{21} = 0.6mm, 0.7mm, 0.8mm, (d) d_{22} = 0.4mm, 0.5mm, 0.6mm. Other parameters are listed in Table 3.

gradient descent or branch and bound may fail to find global extreme values. Besides, the simulated annealing algorithm was also found to be able to find better near-optimal solutions in less computational time compared with other global optimization methods such as genetic algorithm [46]. The above objective function is a complex multi modal function with local minima and maxima, the simulated annealing algorithm is therefore adopted in the present paper. The flow chart of the simulated annealing optimization is shown in Fig. 12. As is shown in Fig. 12, the optimization starts from setting the algorithm control parameters (initial annealing temperature T, final equilibrium temperature T_f, maximum number of iterations L, and cooling factor β) and initializing a solution $\boldsymbol{X}_0$ and an objective value $f(\boldsymbol{X}_0)$. A new solution set is then generated by giving a random perturbation to the initial solution set $\boldsymbol{X} = \boldsymbol{X}_0 + \Delta\boldsymbol{X}$. The current solution set $f(\boldsymbol{X})$ can be accepted directly or with a probability $e^{-(f_0-f)/T}$ based on its comparison with the initial solution $f(\boldsymbol{X}_0)$. The loop will stop when it reaches the maximum iteration number L. The temperature is modified with the cooling factor $T = \beta T$, the outer loop terminates if the current temperature is less than the equilibrium temperature.

5.2. Optimization case study

An optimization case is conducted to prove the feasibility and effectiveness of the proposed optimization strategy. Given the real-world application and manufacturing of the sandwich structures, the constraints of the geometrical parameters are assumed as:

$$\begin{aligned}
&10\text{mm} \le a \le 50\text{mm}\\
&10\text{mm} \le b \le 50\text{mm}\\
&0.1\text{mm} \le t_f \le 3\text{mm}\\
&0.1\text{mm} \le t_c \le 3\text{mm}\\
&0.1\text{mm} \le t_v \le 3\text{mm}\\
&0.2\text{mm} \le d_{11} \le 3\text{mm}\\
&0.2\text{mm} \le d_{12} \le 3\text{mm}\\
&0.2\text{mm} \le d_{21} \le 3\text{mm}\\
&0.2\text{mm} \le d_{22} \le 3\text{mm}
\end{aligned} \tag{12}$$

The core height is assumed as 30 mm, the sandwich structure is also made of resin with a density of 1.117g/cm^3. The algorithm control parameters are defined as $T_i = 1000$, $T_f = 0.1$, $L = 300$, $\beta = 0.9$. The targeted optimization frequency range is $\boldsymbol{\varphi} = [200\ 1600]$Hz. The optimization frequency range can be adjusted according to the noise control needs in engineering applications.

Fig. 13 show the comparison of sound absorption performance and weight of the micro-perforated sandwich structure with NH core before and after optimization. The geometric configurations of the two structures are shown in Table 4. It can be seen from Fig. 13 that the average sound absorption coefficient of the

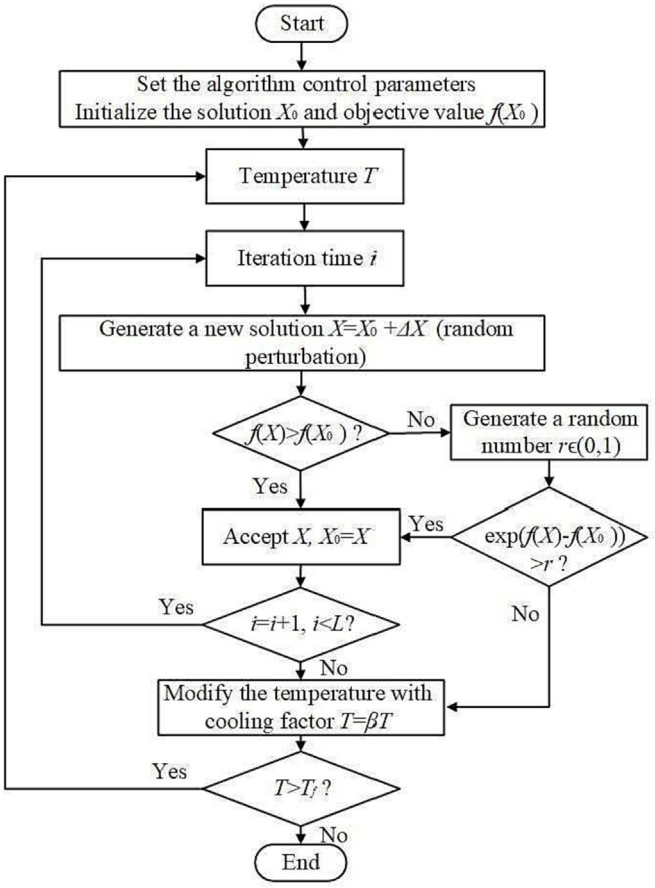

Fig. 12. Flow chart of the optimization procedures based on simulated annealing algorithm.

optimized structure in this range is 0.6083, compared with 0.4334 before optimization, which is a relative increase of 40.36 %. In the meantime, the relative mass M decreases from 32.29 % before optimization to 24.59 % after optimization, with a relative decrease of 23.85 %. Moreover, the sound absorption bandwidth is also extended after optimization. The optimization hence greatly improves the sound absorption performances and reduce the weight of the micro-perforated sandwich structure with NH core.

6. Conclusions

This paper investigated and optimized the sound absorption performances of a novel ultralight multifunctional micro-perforated sandwich structure with N-type hybrid core. The sandwich structure possessed excellent sound absorption performance with as well as mechanical load-bearing capacity and heat transfer capacity. An analytical model was built to calculate the sound absorption of the sandwich structure, which was verified by experimental and numerical methods. The sound absorption mechanisms of the sandwich structure were then explored based on the numerical models, and it found that viscous effect dominated in the energy dissipation. The micro-perforated sandwich structure with NH core was proved to have better sound absorption performance with higher averaged sound absorption over broader frequency range by comparing with other micro-perforated sandwich structures. Since the sound absorption coefficient changed dramatically with the geometrical parameters, an optimization strategy was developed to find out the geometrical parameters that can maximize the sound absorption with minimal weight. The optimized structure showed increased sound absorption value, wider sound absorption band and reduced weight compared with the non-optimal structure. The micro-perforations bring great sound absorption to the sandwich structures with NH core, which could expand the application scope of the structure. The proposed

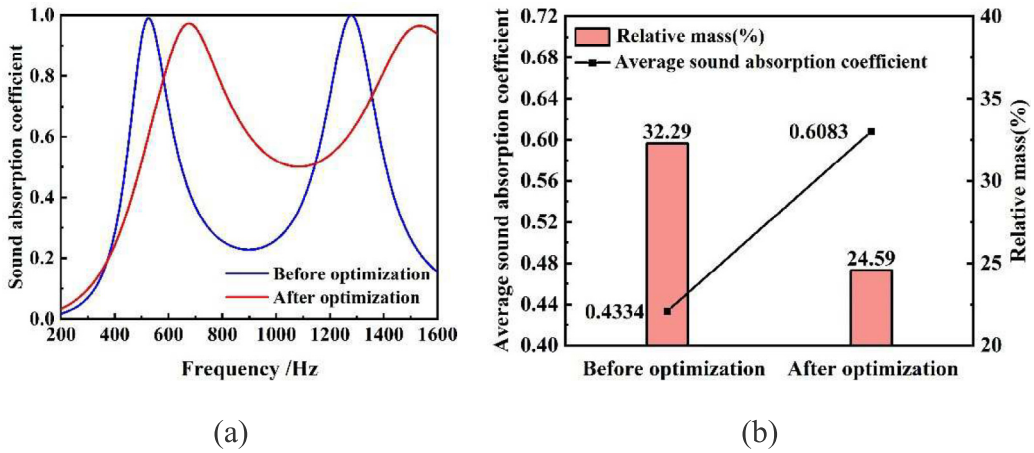

Fig. 13. Comparison between the optimal and non-optimized samples, (a) sound absorption coefficient comparison, (b) average sound absorption coefficient and relative mass comparison.

Table 4
Geometric parameters before and after optimization (/mm).

	a	b	t_f	t_c	t_v	d_{11}	d_{12}	d_{21}	d_{22}
Before optimization	40	6	2	2	2	1.5	1.5	1	1
After optimization	28.6	2.15	2.5	0.5965	1.2	0.9986	1.0345	0.4052	0.3212

method can be also instructive for researchers for the development of multifunctional lightweight structures.

CRediT authorship contribution statement

Yongfeng Jiang: Conceptualization, Methodology, Software. **Cheng Shen:** Validation, Investigation, Supervision. **Han Meng:** Data curation, Writing – original draft. **Wei He:** Resources, Investigation. **Tianjian Lu:** Visualization, Writing – review & editing.

Data availability

Data will be made available on request.

Declaration of Competing Interest

The authors declare that they have no known competing financial interests or personal relationships that could have appeared to influence the work reported in this paper.

Acknowledgement

We would like to acknowledge the support acquired by the National Natural Science Foundation of China under Grant No.12202188 and 12032010, the Research Fund of State Key Laboratory of Mechanics and Control of Mechanical Structures No. MCMS-I-0222K01, and the Fund of Prospective Layout of Scientific Research for NUAA.

References

[1] Bai X, Zheng Z, Nakayama A. Heat transfer performance analysis on lattice core sandwich panel structures. Int J Heat Mass Trans 2019;143:118525.
[2] Haldar S, Bruck HA. Mechanics of composite sandwich structures with bioinspired core. Compos Sci Technol 2014;95:67–74.
[3] Queheillalt DT, Carbajal G, Peterson G, Wadley HN. A multifunctional heat pipe sandwich panel structure. Int J Heat Mass Trans 2008;51:312–26.
[4] Sun Y, Guo LC, Wang TC, Zhong SY, Pan HZ. Bending behavior of composite sandwich structures with graded corrugated truss cores. Compos Struct 2018;185:446–54.
[5] Tarlochan F. Sandwich structures for energy absorption applications: A review. Materials 2021;14:4731.
[6] Sarvestani HY, Akbarzadeh A, Mirbolghasemi A, Hermenean K. 3D printed meta-sandwich structures: Failure mechanism, energy absorption and multi-hit capability. Mater Design 2018;160:179–93.
[7] Zhu F, Lu G, Ruan D, Wang Z. Plastic deformation, failure and energy absorption of sandwich structures with metallic cellular cores. Int J Prot Struct 2010;1:507–41.
[8] Liu J, Xiang L, Kan T. The effect of temperature on the bending properties and failure mechanism of composite truss core sandwich structures. Compos Part A-Appl S 2015;79:146–54.
[9] Birman V, Kardomateas GA. Review of current trends in research and applications of sandwich structures. Compos Part B-Eng 2018;142:221–40.
[10] Palomba G, Epasto G, Crupi V. Lightweight sandwich structures for marine applications: a review. Mech Adv Mater Struct 2021:1–26.
[11] Feng Y, Qiu H, Gao Y, Zheng H, Tan J. Creative design for sandwich structures: A review. Int J Adv Robot Syst 2020;17:1729881420921327.
[12] Zinno A, Fusco E, Prota A, Manfredi G. Multiscale approach for the design of composite sandwich structures for train application. Compos Struct 2010;92:2208–19.
[13] Mead DJ. Free wave propagation in periodically supported, infinite beams. J Sound Vib 1970;11:181–97.
[14] Mead DJ, Pujara KK. Space-harmonic analysis of periodically supported beams: response to convected random loading. J Sound Vib 1971;14:525–41.
[15] Sorokin SV. Vibrations of and sound radiation from sandwich plates in heavy fluid loading conditions. Compos Struct 2000;48:219–30.
[16] Mead DJ. Plates with regular stiffening in acoustic media: vibration and radiation. J Acoust Soc Am 1990;88:391–401.
[17] Kazemahvazi S, Zenkert D. Corrugated all-composite sandwich structures. Part 1: Modeling. Compos Sci Technol 2009;69:913–9.
[18] Kazemahvazi S, Tanner D, Zenkert D. Corrugated all-composite sandwich structures. Part 2: Failure mechanisms and experimental programme. Compos Sci Technol 2009;69:920–5.
[19] Ge L, Zheng HY, Li HM, Liu BS, Su HR. Fang DN Compression behavior of a novel sandwich structure with bi-directional corrugated core. Thin-Walled Struct 2021;161:107413.
[20] Zhao CY, Lu TJ. Analysis of microchannel heat sinks for electronics cooling. Int J Heat Mass Trans 2002;45:4857–69.
[21] Côté F, Deshpande V, Fleck N, Evans A. The compressive and shear responses of corrugated and diamond lattice materials. Int J Solids Struct 2006;43:6220–42.
[22] Sun S, Liu D, Sheng YL, Feng SS, Zhu HB, Lu TJ. Out-of-plane compression of a novel hybrid corrugated core sandwich panel. Compos Struct 2021;272:114222.
[23] Sun S, Feng S, Zhang Q, Lu TJ. Forced convection in additively manufactured sandwich-walled cylinders with thermo-mechanical multifunctionality. Int J Heat Mass Trans 2020;149:119161.
[24] Li Y, Zhang F, Sunden B, Xie G. Laminar thermal performance of microchannel heat sinks with constructal vertical Y-shaped bifurcation plates. Appl Therm Eng 2014;73:185–95.
[25] Lorenzini G, Biserni C, Isoldi LA, Dos Santos ED, Rocha LAO. Constructal design applied to the geometric optimization of Y-shaped cavities embedded in a conducting medium. J Electron Packaging 2011;133:041008.
[26] Lorenzini G, Biserni C, Estrada ED, Isoldi LA, Dos Santos ED, Rocha LAO. Constructal design of convective Y-shaped cavities by means of genetic algorithm. J Heat Transf-T ASME 2014;136(7).
[27] Maa DY. Theory and design of microperforated panel sound-absorbing constructions. Sci China Ser A-Math 1975;18:55–71.
[28] Allam S, Åbom M. A new type of muffler based on microperforated tubes. J Vib Acoust 2011;133(3).
[29] Fuchs HV, Zha X. Micro-perforated structures as sound absorbers–a review and outlook. Acta Acust United Acust 2006;92:139–46.
[30] Herrin D, Liu J, Seybert A. Properties and applications of microperforated panels. Sound Vib 2011;45:6–9.
[31] Sakagami K, Yairi M, Morimoto M. Multiple-leaf sound absorbers with microperforated panels: an overview. Acoust Aust 2010;38:76–81.
[32] Sakagami K, Morimoto M, Yairi M. Application of microperforated panel absorbers to room interior surfaces. Int J Acoust Vib 2008;13:120–4.
[33] Hou J, Zhu H, Yuan S, Liao J. Sound transmission characteristics of underwater flexible micro-perforated panels. Appl Acoust 2021;181:108165.
[34] Kim HS, Ma PS, Ki BK, Kim SR, Seo YH. Underwater sound absorption and insulation of elastic micro-perforated plates in impedance tubes. Appl Acoust 2022;197:108935.
[35] Dupont T, Pavic G, Laulagnet B. Acoustic properties of lightweight micro-perforated plate systems. Acta Acust United Acust 2003;89:201–12.
[36] Bravo T, Maury C, Pinhède C. Enhancing sound absorption and transmission through flexible multi-layer micro-perforated structures. J Acoust Soc Am 2013;134:3663–73.
[37] Bravo T, Maury C, Pinhède C. Sound absorption and transmission through flexible micro-perforated panels backed by an air layer and a thin plate. J Acoust Soc Am 2012;131:3853–63.
[38] Meng H, Galland MA, Ichchou M, Bareille O, Xin FX, Lu TJ. Small perforations in corrugated sandwich panel significantly enhance low frequency sound absorption and transmission loss. Compos Struct 2017;182:1–11.
[39] Meng H, Galland MA, Ichchou M, Xin FX, Lu TJ. On the low frequency acoustic properties of novel multifunctional honeycomb sandwich panels with micro-perforated faceplates. Appl Acoust 2019;152:31–40.
[40] Tang YF, Li F, Xin FX, Lu TJ. Heterogeneously perforated honeycomb-corrugation hybrid sandwich panel as sound absorber. Mater Design 2017;134:502–12.
[41] Tang YF, Ren S, Meng H, Xin FX, Huang L, Chen T, et al. Hybrid acoustic metamaterial as super absorber for broadband low-frequency sound. Sci Rep 2017;7:43340.
[42] Tang YF, Xin FX, Lu TJ. Sound absorption of micro-perforated sandwich panel with honeycomb-corrugation hybrid core at high temperatures. Compos Struct 2019;226:111285.
[43] He W, Peng XJ, Xin FX, Lu TJ. Ultralight micro-perforated sandwich panel with hierarchical honeycomb core for sound absorption. J Sandw Struct Mater 2021;24:201–17.
[44] Maa DY. Potential of microperforated panel absorber. J Acoust Soc Am 1998;104:2861–6.
[45] Zhang ZM, Gu XT. The theoretical and application study on a double layer microperforated sound absorption structure. J Sound Vib 1998;215:399–405.
[46] Ghazanfari M, Alizadeh S, Fathian M, Koulouriotis DE. Comparing simulated annealing and genetic algorithm in learning FCM. Appl Math Comput 2007;192:56–68.